PI-Specific Phospholipase C Cleavage of a Reconstituted GPI-Anchored Protein: Modulation by the Lipid Bilayer†

Marty T. Lehto and Frances J. Sharom*

Guelph-Waterloo Centre for Graduate Work in Chemistry and Biochemistry, Department of Chemistry and Biochemistry, University of Guelph, Guelph, Ontario, Canada N1G 2W1

Received July 30, 2001; Revised Manuscript Received November 2, 2001

ABSTRACT: Release of glycosylphosphatidylinositol- (GPI-) anchored ectoenzymes from the membrane by phosphatidylinositol- (PI-) specific phospholipases may play an important role in modulating the surface expression and function of this group of proteins. To investigate how the properties of the host membrane affect anchor cleavage, porcine lymphocyte ecto-5′-nucleotidase (5′-NTase; EC 3.1.3.5) was purified, reconstituted into lipid bilayer vesicles of various lipids, and cleaved using PI-PLC from *Bacillus thuringiensis* (*Bt*-PI-PLC). *Bt*-PI-PLC activity was highly dependent on the chain length and unsaturation of the constituent phospholipids. Very high rates of cleavage were observed in fluid lipids with a low phase transition temperature (T_m), in lymphocyte plasma membrane, and in a lipid mixture that formed rafts. Arrhenius plots of the rate of anchor cleavage in various lipids showed a characteristic break at the bilayer T_m, together with a discontinuity close to T_m. The activation energy for GPI anchor cleavage was substantially higher in gel phase bilayers compared to those in the liquid crystalline phase. The addition of cholesterol simultaneously abolished the phase transition and the large difference in cleavage rates observed above and below T_m. Inclusion of GM_1 and GT_{1b} (components of lipid rafts) in the bilayer reduced the overall activity, but the pattern of the Arrhenius plots remained unchanged. Both gangliosides had similar effects, suggesting that bilayer surface charge has little influence on PI-PLC activity. Taken together, these results suggest that lipid fluidity and packing are the most important modulators of *Bt*-PI-PLC activity on GPI anchors.

A wide variety of proteins are anchored to the external surface of eukaryotic cells by a glycosylphosphatidylinositol (GPI)[1] anchor, including extracellular coat proteins, hydrolytic enzymes, adhesion proteins, surface antigens, and receptors (*1*−*4*). The GPI anchor appears to play a role in the increased lateral mobility of some plasma membrane proteins (*5*), the intracellular targeting of proteins in polarized epithelial cells (*6*), and secretory granule biogenesis (*7*). In addition, the GPI anchor is responsible for the clustering of this class of proteins into glycosphingolipid-enriched lipid rafts that are resistant to extraction by nonionic detergents (*8*, *9*). Lipid rafts appear to be "hot spots" or platforms for signal transduction through a large number of cellular receptors (*10*−*12*), such as those in cells of the immune system (*13*). Rafts and/or GPI-anchored proteins also appear to be targets for bacterial invasion and entry into the cell of bacterial toxins such as aerolysin (*14*, *15*).

The GPI anchor can be cleaved by phospholipases C and D, which release the protein in soluble form and thus remove it from the cell surface. Cleavage by endogenous phospholipases likely represents an important means of regulating the surface expression and function of this class of proteins. Intracellular phosphatidylinositol-specific phospholipase C (PI-PLC; EC 3.1.4.11) catalyzes the cleavage of phosphatidylinositol 4,5-bisphosphate to produce diacylglycerol (DAG) and *myo*-inositol phosphates in mammalian cells (*16*). The production of DAG (responsible for the activation of protein kinase C) and inositol 1,4,5-trisphosphate (responsible for intracellular calcium mobilization) by PI-PLC is an important factor in PI-mediated signaling pathways. Extracellular PI-PLC is secreted by several microorganisms (*17*−*19*) although the exact physiological function of the enzyme is unclear. Bacterial PI-PLC catalyzes the hydrolysis of membrane-bound phosphatidylinositol (PI) to yield DAG and *myo*-inositol 1,2-(cyclic)-phosphate (cIP). The same enzyme slowly hydrolyzes the water-soluble cIP to D-*myo*-inositol 1-phosphate. Bacterial PI-PLCs appear to play an essential role as virulence factors in several pathogenic strains, including *Staphylococcus aureus* (*20*) and *Listeria monocy-*

† This work was supported by a grant to F.J.S. from the Natural Sciences and Engineering Research Council of Canada.

* To whom correspondence should be addressed: Department of Chemistry and Biochemistry, University of Guelph, Guelph, Ontario, Canada N1G 2W1. Telephone: (519) 824-4120 ext 2247. Fax: (519) 766-1499. E-mail: sharom@chembio.uoguelph.ca.

[1] Abbreviations: BSA, bovine serum albumin; CHAPS, 3-[(3-cholamidopropyl)dimethylammonio]-1-propanesulfonate; cIP, *myo*-inositol 1,2-(cyclic)-phosphate; DAG, diacylglycerol; DiCP, dicetyl phosphate; DMPC, dimyristoylphosphatidylcholine; DOPC, dioleoylphosphatidylcholine; DSC, differential scanning calorimetry; GPI, glycosylphosphatidylinositol; GPI-PLD, glycosylphosphatidylinositol-specific phospholipase D; Hepes, *N*-(2-hydroxyethyl)piperazine-*N*′-2-ethanesulfonic acid; IBS, interfacial binding surface; 5′-NTase, ecto-5′-nucleotidase; PC, phosphatidylcholine; PI, phosphatidylinositol; *Bt*-PI-PLC, phosphatidylinositol-specific phospholipase C from *Bacillus thuringiensis*; PE, phosphatidylethanolamine; PMPC, palmitoylmyristoylphosphatidylcholine; SA, stearylamine; SCRL, sphingolipid/cholesterol-rich liposomes; SM, sphingomyelin; SOPC, stearoyloleoylphosphatidylcholine.

10.1021/bi011579w CCC: $22.00
Published on Web 12/29/2001

togenes (*21*, *22*), possibly because of their ability to cleave the GPI anchor of mammalian membrane proteins. Bacterial PI-PLCs have proven to be extremely useful tools in identifying and characterizing GPI anchors and in examining the behavior of GPI-anchored proteins in membranes.

Water-soluble phospholipase enzymes tend to be more active toward an aggregated substrate. This phenomenon, termed "interfacial activation", depends on the physicochemical nature as well as the organization and dynamics of the interface and has been studied quite extensively for phospholipase A_2 (reviewed in refs *23* and *24*) and other phospholipases (*25*). Bacterial PI-PLC displays interfacial activation toward both the membrane-bound substrate PI (*26*, *27*) and the water-soluble substrate cIP (*28*, *29*); however, little is known about the interfacial kinetics of bacterial PI-PLC cleavage of GPI-anchored proteins in lipid bilayer vesicles. Recent work in our laboratory explored the catalytic activation of a purified GPI-anchored protein, 5′-nucleotidase (5′-NTase), following cleavage of the GPI anchor by PI-PLC from *Bacillus thuringiensis* (*Bt*-PI-PLC) (*30*). Results showed that the physicochemical properties of the membrane can modulate both the extent of catalytic activation observed on anchor removal and the susceptibility of the anchor to phospholipase cleavage.

The use of GPI-anchored proteins in reconstituted lipid bilayer systems provides a powerful means to control precisely the composition and biophysical properties of the membrane environment and examine their effects on the activity of phospholipase enzymes. In the present study, the kinetics of cleavage of a GPI anchor by *Bt*-PI-PLC were examined in defined lipid bilayer vesicles. The GPI-anchored ectoenzyme, 5′-NTase, was chosen as the target for cleavage, since it is widely distributed in higher eukaryotes, and has been successfully purified and reconstituted in our laboratory. This study represents the first to use a kinetic approach to examine the effects on PI-PLC anchor cleavage activity of membrane surface charge, lipid fluidity and phase state, and the presence of lipid raft components. Results showed that membrane fluidity and packing were the most important factors affecting GPI anchor cleavage by *Bt*-PI-PLC.

MATERIALS AND METHODS

Materials. Egg phosphatidylethanolamine (PE), egg phosphatidylcholine (PC), dimyristoylphosphatidylcholine (DMPC), palmitoylmyristoylphosphatidylcholine (PMPC), dioleoylphosphatidylcholine (DOPC), stearoyloleoylphosphatidylcholine (SOPC), and galactocerebrosides (type II from bovine brain) were supplied by Avanti Polar Lipids (Alabaster, AL). GM_1 and GT_{1b}, 3-[(3-cholamidopropyl)dimethylammonio]-1-propanesulfonate (CHAPS), sphingomyelin (SM, from bovine erythrocytes and bovine brain), cholesterol, dicetyl phosphate (DiCP), stearylamine (SA), and Triton X-114 were purchased from Sigma Chemical Co. (St. Louis, MO). Recombinant *B. thuringiensis* PI-PLC (250−300 units/mL; expressed in *Bacillus subtilis*) was obtained from Oxford GlycoSciences Inc. (Bedford, MA). One unit of enzyme activity released 1 μmol of P_i from phosphatidylinositol per minute at 37 °C, pH 7.5.

5′-NTase Purification and Reconstitution. 5′-NTase was isolated from porcine mesenteric lymph nodes as previously described (*30*). Briefly, fresh lymph nodes were obtained within a few minutes of slaughter and either used fresh or quick-frozen in liquid nitrogen and stored at −70 °C. Plasma membrane vesicles were prepared according to the method of Maeda et al. (*31*). Plasma membrane vesicles were solubilized in 50 mM CHAPS, and 5′-NTase was purified using two sequential affinity chromatography steps, the first on lentil lectin−Sepharose 4B (Pharmacia Canada, Baie d'Urfé, QC) and the second on 5′-AMP−Sepharose (Sigma Chemical Co., St. Louis, MO). Fractions containing 5′-NTase activity were combined and dialyzed extensively against 10 mM ammonium bicarbonate buffer, pH 7.4, followed by lyophilization to dryness. The lyophilized enzyme was redissolved in 12.5 mM CHAPS in 50 mM Tris-HCl/150 mM NaCl (pH 7.4). The protein content of the concentrated 5′-NTase sample was determined by the method of Peterson (*32*).

Reconstitution of 5′-NTase into Lipid Bilayer Vesicles. Purified 5′-NTase was reconstituted into lipid bilayer vesicles using a modification of the detergent dialysis technique described previously (*33*−*35*). A mixture of the desired lipids (1−3 mg) in MeOH−$CHCl_3$ was evaporated to dryness in a small glass tube using N_2 gas. Brain cerebrosides were dissolved in pyridine to avoid $CHCl_3$ according to the manufacturer's instructions (Avanti Polar Lipids). Lipid mixtures were pumped under vacuum for 1 h to remove all traces of organic solvent. The dried lipid was dissolved in 12.5 mM CHAPS in 50 mM Tris-HCl, 0.1 M NaCl, 0.2 mM dithiothreitol, 0.02% (w/v) sodium azide, 0.7 mM $CaCl_2$, 0.7 mM $MgCl_2$, and 0.7 mM $MnCl_2$ (pH 7.4) and mixed with purified concentrated 5′-NTase in the same buffer. The detergent was removed by dialysis in Spectrapor 4 tubing (12−14 kDa cutoff) against three changes (a total of 3 L) of 20 mM Tris-HCl buffer (pH 7.4). Following dialysis, lipid vesicles were harvested by centrifugation (41000*g* for 10 min) and then resuspended in 50 mM Tris-HCl, 0.15 M NaCl, and 0.02% sodium azide, pH 7.4 (TBS buffer). The resulting lipid bilayer vesicles had a final lipid:protein ratio of 150−200:1 (w/w) for vesicles containing 5′-NTase. Purified 5′-NTase was reconstituted into the following lipid systems: DMPC, egg PC, DOPC, SOPC, PMPC, sphingolipid/cholesterol-rich liposomes (SCRL; consisting of egg PC:egg PE:SM:cerebrosides:cholesterol, 1:1:1:1:2 mole ratio) (*36*), DMPC containing 5% (w/w) of the gangliosides GM_1 or GT_{1b}, DMPC containing 5% GM_1/22% cholesterol (w/w/w), DMPC containing 5% (w/w) DiCP, and DMPC containing 5% (w/w) SA. Thy-1 was coreconstituted with 5′-NTase using dialysis membrane with a 3.5 kDa cutoff. Vesicles containing Thy-1 and 5′-NTase had a final lipid:protein ratio of 9.5:1 (w/w). Rat brain Thy-1 was purified as described previously (*37*).

The size range for the different reconstituted vesicle systems was determined using dynamic light scattering (*37*). All are LUVs with a bimodal distribution of vesicle sizes falling in the range 100−350 nm for the smaller population and 330−900 nm for the larger population.

Cleavage of 5′-NTase by PI-Specific Phospholipase C. We and others have previously shown that when *Bt*-PI-PLC was used at low protein concentrations, it was inactivated in a time-dependent fashion (*35*, *38*). This loss of activity could be completely prevented by addition of 1% (w/v) BSA, which was, therefore, included in all of the cleavage reaction mixtures. An aliquot (20 μL) of membrane-bound 5′-NTase

in TBS supplemented with 1% (w/v) BSA (TBS/BSA buffer) was made up to 50 μL with *Bt*-PI-PLC in the same buffer at the indicated temperature for the appropriate amount of time. Two negative controls and one positive control were also assayed for each *Bt*-PI-PLC concentration used. One negative control and the positive control had TBS/BSA buffer added in place of *Bt*-PI-PLC at $t = 0$, and the second negative control had *Bt*-PI-PLC added at the end of the experiment, just before the reaction was stopped. The GPI-anchored form of 5′-NTase in CHAPS was separated from the soluble form by two-phase separation in Triton X-114, based on a modification of the method of Bordier (*39*). After the indicated time period, the cleavage reaction was stopped by the addition of 50 μL of ice-cold 20% (v/v) Triton X-114 in TBS buffer (50 μL of TBS was added to the positive control). The mixture was cooled on ice for 3 min, warmed to 37 °C for 3 min, and then centrifuged at 14700*g* for 3 min at room temperature (the positive control was not centrifuged). The upper aqueous phase ($2-3 \times 20$ μL aliquots) was then assayed for the cleaved anchorless form of 5′-NTase. The enzymatic activity of 5′-NTase was determined by measuring the release of [2-^{3}H]adenosine from 5′-[2-^{3}H]AMP as described previously (*30*, *33*, *35*).

For detergent-solubilized 5′-NTase, cleavage experiments were performed as described above, except that special precautions (described below) had to be taken for the Triton X-114 extraction step because the CHAPS content of the sample interfered with the cloud point of Triton X-114. At the end of the cleavage reaction, 100 μL (instead of 50 μL) of ice-cold 20% (v/v) Triton X-114 was added (100 μL of TBS buffer was added to the positive control), and the samples were cooled on ice for 3 min, warmed to 37 °C for 3 min, and then centrifuged at 14700*g* for 3 min at 37 °C (instead of room temperature) in a microcentrifuge to separate the phases. The upper aqueous phase was assayed for the cleaved soluble form of 5′-NTase as indicated above.

Kinetic Analysis of 5′-NTase Release. The initial rate of cleavage by *Bt*-PI-PLC of purified 5′-NTase reconstituted into bilayer vesicles of various purified phospholipids, or purified 5′-NTase in CHAPS, was determined over the linear period of the reaction (see Results). For collection of Arrhenius plot data, the initial rate of release of 5′-NTase was measured at temperatures in the range 17−33 °C (±0.1 °C), with the appropriate concentration of *Bt*-PI-PLC, using an assay time of 40 min. The experimental data were transformed into Arrhenius plots, and the slopes of the lines were obtained using linear regression with the Marquardt−Levenberg algorithm (SigmaPlot, SPSS Inc., Chicago, IL). Arrhenius plots were used to analyze the effects of lipid phase state on the cleavage of 5′-NTase by *Bt*-PI-PLC. The Arrhenius equation postulates that the temperature dependence of any reaction rate can be described by the equation:

$$\ln k = \ln A - (E_{act}/RT)$$

where E_{act}, the activation energy, corresponds to the standard enthalpy of activation, and ln A is a constant. A plot of log k vs $1/T$ (Arrhenius plot) is a straight line with slope $-E_{act}/2.303R$. According to classical kinetic theory, the constant $A = PZ$, where Z is the frequency of molecular collisions for a bimolecular reaction and P is the probability that the two molecules are correctly oriented for a reaction to take place. According to transition state theory, the constant A is related to the activation entropy, $\Delta S^{\ddagger}$, as follows:

$$\Delta S^{\ddagger} = R \ln(ANh/RT) - R$$

Detergent Resistance of Reconstituted Lipid Bilayer Membranes. An aliquot (135 μL) of 5′-NTase in lipid vesicles was mixed with an equal volume of 2% (v/v) Triton X-100 to give a final concentration of 1% (v/v). Following incubation on ice for 30 min, the sample volume was made up to 800 μL with 60% (w/v) sucrose to give a final sucrose content of 40% (w/v). The sample was then placed at the bottom of a 5.2 mL ultracentrifuge tube and overlayed with 30% (w/v) sucrose (2.2 mL) followed by 5% (w/v) sucrose (2.2 mL). Following centrifugation at 64000*g* for 3 h, 400 μL fractions (a total of 13) were collected from the top of the tube and assayed for 5′-NTase activity. Low-density insoluble lipid material floated at the interface between the 5% and 30% sucrose layers and was collected in fractions 2−8, whereas completely soluble and high-density insoluble material remained in the 40% sucrose layer and was collected in fractions 10−13. Fractions 2−8 were referred to as detergent-resistant membranes (DRMs).

Differential Scanning Calorimetry. A Microcal MC-2 high-sensitivity differential scanning calorimeter (Microcal Inc., Northampton, MA) was used to obtain calorimetric data on the gel-to-liquid crystalline phase transition for the different lipid systems tested. Lipid vesicles (3 mg of lipid) in 3 mL of TBS were prewarmed above the gel to phase transition temperature prior to calorimetric analysis and then cooled to 4 °C. The lipid samples were analyzed at a scanning rate of 1.5 °C/min, and each sample was scanned at least twice up to 40 °C, with highly reproducible results. Typically, the T_m values obtained for the various samples were within 0.22−0.24 °C of each other. The calorimetric data were analyzed using Microcal Origin Scientific software (Microcal Software Inc.). The phase transition (melting) temperature of the bilayer, T_m, was defined as the temperature at the peak maximum.

RESULTS

Kinetics of Cleavage of 5′-NTase by Bt-PI-PLC. In previous work in our laboratory, the EC_{50} (the concentration of *Bt*-PI-PLC required to release 50% of the 5′-NTase in soluble form) was used to give an estimate of the ability of *Bt*-PI-PLC to cleave the GPI anchor of 5′-NTase (*30*). Results showed that EC_{50} values varied over a range of almost 200-fold (see Table 1), depending on the lipid chosen for reconstitution. One of the objectives of the current work was to further investigate the ability of *Bt*-PI-PLC to cleave the 5′-NTase anchor using a more precise approach, by looking at the initial rates of cleavage in different lipid systems. Figure 1A shows that the initial rate of cleavage of 5′-NTase was linear up to at least 40 min for both porcine lymphocyte plasma membrane vesicles and purified 5′-NTase reconstituted into proteoliposomes composed of various lipids. The initial rate of cleavage followed a pattern similar to that of the EC_{50} data, in that a high EC_{50} was associated with a low initial rate of cleavage (Table 1). The initial rates of cleavage were highest for 5′-NTase in porcine lymphocyte plasma membrane vesicles, SCRL, and egg PC (which also had a low EC_{50}) and substantially lower in DMPC (which had a

Table 1: *Bt*-PI-PLC-Mediated Cleavage of Membrane-Bound 5′-NTase at 37 °C in Different Lipid Environments[a]

lipid environment	EC_{50} (unit/mL)	initial rate [% cleaved/ (milliunit of *Bt*-PI-PLC·min)]
lymphocyte plasma membrane vesicles	0.03	180 ± 7
SCRL	0.01	56 ± 6
egg PC	0.008	27 ± 1
PMPC	ND[b]	0.13 ± 0.01
DMPC	0.7	0.96 ± 0.13
SOPC	ND	17.9 ± 3.2
DOPC	ND	37 ± 1

[a] The initial rates were calculated from the slopes of the lines in Figures 1A and 2. The error indicates the goodness of fit to a straight line by linear regression analysis. The EC_{50} values, defined as the concentration of *Bt*-PI-PLC required to release 50% of the 5′-NTase in soluble form after a 90 min incubation at 37 °C, are taken from ref *30*. [b] ND, not determined.

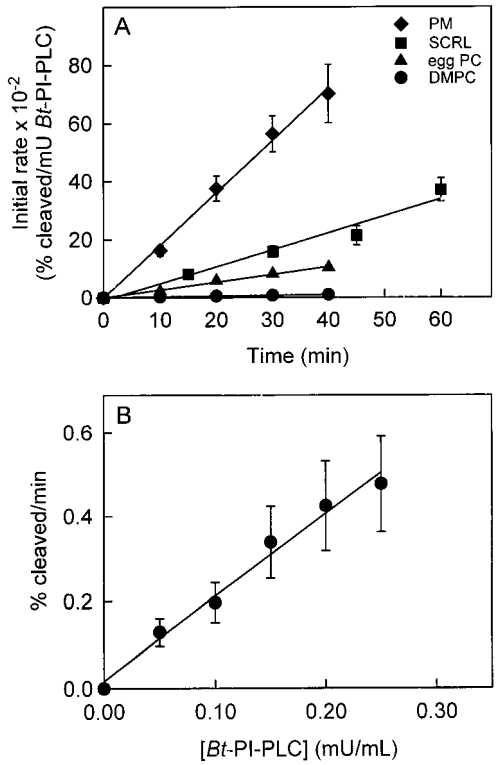

FIGURE 1: Cleavage of the 5′-NTase GPI anchor by *Bt*-PI-PLC. (A) Initial rates of cleavage of 5′-NTase. Lymphocyte plasma membrane vesicles (PM, ◆) and purified 5′-NTase reconstituted into proteoliposomes of SCRL (■), egg PC (▲), and DMPC (●) were incubated with *Bt*-PI-PLC at 37 °C for various times. Cleaved 5′-NTase was separated from the membrane-bound form by Triton X-114 phase partitioning as described in Materials and Methods, and the enzyme activity was determined. Data points represent the mean ± SEM ($n = 3$). (B) Dependence of the rate of GPI anchor cleavage on phospholipase concentration. Lymphocyte plasma membrane vesicles were incubated with increasing concentrations of *Bt*-PI-PLC at 37 °C for 30 min. The cleaved form of 5′-NTase was separated from the membrane-bound form by Triton X-114 phase partitioning, followed by measurement of the enzyme activity. The data are presented as the percent cleaved per minute over the 30 min period. Data points represent the mean ± SEM ($n = 3$).

high EC_{50}). In any kinetic study, it is also important to test whether the initial rates of activity of an enzyme are linear with respect to the concentration of the enzyme. Figure 1B shows the initial rate of cleavage of 5′-NTase with increasing concentrations of *Bt*-PI-PLC in porcine lymphocyte plasma membrane vesicles. The results showed that the cleavage of 5′-NTase was linear with respect to *Bt*-PI-PLC concentration. This experiment was repeated for the other reconstituted 5′-NTase samples used in this study, and all showed linearity with *Bt*-PI-PLC concentration (data not shown).

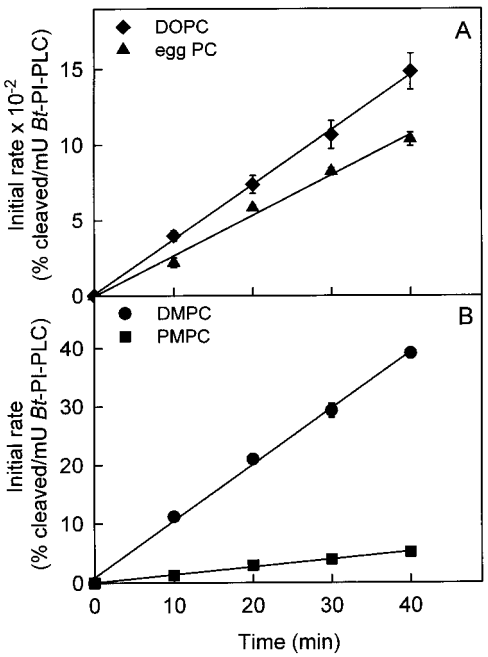

FIGURE 2: Effect of acyl chain length and unsaturation on the initial rate of *Bt*-PI-PLC cleavage of 5′-NTase in PC proteoliposomes. Initial rates of cleavage of 5′-NTase by *Bt*-PI-PLC at 37 °C in vesicles of DOPC (◆), egg PC (▲), DMPC (●), and PMPC (■). Data points represent the mean ± SEM ($n = 2$); where not visible, error bars are included within the symbols.

Effect of Acyl Chain Length and Unsaturation on Bt-PI-PLC Cleavage of 5′-NTase. The initial rates of *Bt*-PI-PLC cleavage of 5′-NTase were examined in proteoliposomes composed of several different phosphatidylcholines. Figure 2 shows that there was a substantial difference in the rate of cleavage depending on acyl chain length and unsaturation. The initial rates of cleavage varied over a range of ∼280-fold for the different PC species tested (Table 1). The two lipid systems with the lowest initial rate of cleavage were those with saturated acyl chains, DMPC and PMPC, at 0.96% and 0.13% cleaved/(milliunit of *Bt*-PI-PLC·min), respectively. PMPC differs from DMPC in that one acyl chain is only two carbon atoms longer, yet the initial rate of cleavage was substantially lowered by >7-fold. Clearly, lipid chain length has a dramatic effect on anchor cleavage by *Bt*-PI-PLC.

The two PC species with substantially higher initial rates of anchor cleavage were those with unsaturated acyl chains. Egg PC is composed of ∼45% mono-, di-, and polyunsaturated acyl chains of primarily 16 and 18 carbon atoms (Avanti Polar Lipids, Alabaster AL), whereas DOPC has two monounsaturated 18 carbon chains. The initial rates of cleavage were 27% and 37% cleaved/(milliunit of *Bt*-PI-PLC·min) for egg PC and DOPC, respectively (Table 1). This represents an ∼27-fold increase in the initial rate of cleavage for egg PC and an ∼38-fold increase for DOPC, compared to DMPC, which has completely saturated acyl chains. Thus, the presence of unsaturated acyl chains has a dramatic effect on GPI anchor cleavage by *Bt*-PI-PLC by

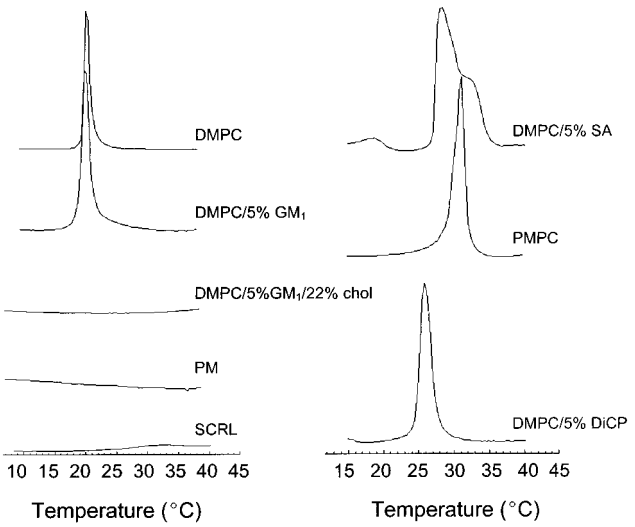

FIGURE 3: Melting transitions of lipids used in this study. Bilayers composed of various lipids and lipid mixtures were subjected to DSC analysis to determine the phase transition temperature, T_m. Samples (1 mg/mL lipid) were prewarmed to 40 °C, cooled to 4 °C, and thermally analyzed at a scan rate of 1.5 °C/min. Duplicate scans of the same sample were essentially superimposable.

substantially increasing the initial rate of cleavage when compared to lipid bilayer vesicles with saturated acyl chains. The initial rate of cleavage correlates well with the T_m of the lipids. The lipid with the highest initial rate, DOPC, had the lowest melting temperature, T_m (−20 °C), followed by egg PC (−10 °C), SOPC (6 °C), DMPC (24 °C; Figure 3), and PMPC (30.5 °C; Figure 3). These results suggest that *Bt*-PI-PLC prefers lipids with a low T_m, and the rate of GPI anchor cleavage appears to be directly related to lipid fluidity.

Effect of Lipid Bilayer Surface Charge on the Cleavage of 5′-NTase by PI-PLC. Previous work in our laboratory suggested that membrane surface charge may affect the ability of PI-PLC to cleave the GPI anchor (*35*). A goal of this study was to further investigate this phenomenon by measuring the initial rates of *Bt*-PI-PLC cleavage of 5′-NTase in bilayers containing charged species. 5′-NTase was reconstituted into DMPC bilayers containing either negatively charged DiCP (16 carbon chain) or positively charged SA (18 carbon chain). At 20 °C, when the lipid bilayer is in the gel phase, inclusion of DiCP in the bilayer increased the rate of anchor cleavage by *Bt*-PI-PLC by ∼2-fold, whereas inclusion of SA slightly reduced activity (Table 2). In the liquid crystalline phase (37 °C), similar trends were observed, although positively charged SA led to a much larger (∼4-fold) reduction in the initial rate of anchor cleavage (Table 2).

These results initially suggested that membrane surface charge may affect the ability of *Bt*-PI-PLC to cleave the GPI anchor. A positive surface charge appeared to reduce the efficiency of anchor cleavage whereas a negative surface charge slightly increased the rate of anchor cleavage. These small effects of surface charge may arise from the presence of a single Lys residue within the enzyme region that is believed to interact with the membrane surface (see Discussion). However, bilayer fluidity and packing likely also play a role in the effects of DiCP and SA on anchor cleavage, since there is a difference in the observed degree of activation or inhibition depending on whether DMPC is in the rigid

Table 2: Effect of Various Components on *Bt*-PI-PLC Cleavage of the 5′-NTase GPI Anchor in DMPC Bilayers[a]

	initial rate [% cleaved/(milliunit of *Bt*-PI-PLC·min)]	
	20 °C	37 °C
DMPC	0.039 ± 0.002	0.98 ± 0.10
DMPC + 5% (w/w) DiCP	0.085 ± 0.005	1.46 ± 0.13
DMPC + 5% (w/w) SA	0.034 ± 0.002	0.24 ± 0.01
DMPC + 5% (w/w) GM_1	0.083 ± 0.009	0.22 ± 0.01
DMPC + 5% (w/w) GT_{1b}	0.092 ± 0.007	0.25 ± 0.01
DMPC + 5% (w/w) GM_1 + 22% (w/w) cholesterol	0.27 ± 0.01	0.38 ± 0.01
DMPC + 10:1 (w/w) Thy-1	0.027 ± 0.002	0.56 ± 0.15

[a] 5′-NTase reconstituted into DMPC bilayers containing different components was incubated with *Bt*-PI-PLC for 15 min at 20 or 37 °C. Data are presented as the mean ± SEM (n = 4).

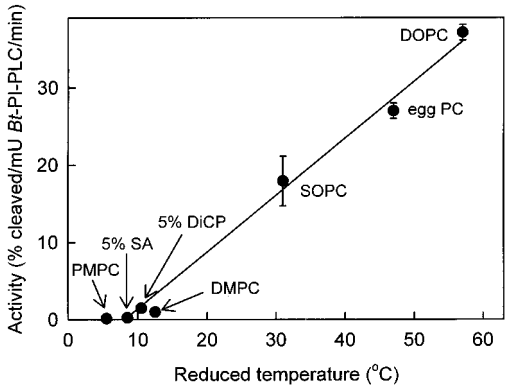

FIGURE 4: Correlation of the reduced temperature of the bilayer phase transition with the activity of *Bt*-PI-PLC. The initial rates of phospholipase cleavage of 5′-NTase in different PC bilayers (from Tables 1 and 2) were plotted against the reduced temperature, which is defined as the temperature of the cleavage assay (37 °C) minus the T_m of the lipid bilayer. Data points represent the mean ± SEM (n = 3); where not visible, error bars are included within the symbols.

gel phase (20 °C) or the fluid liquid crystalline phase (37 °C). Differential scanning calorimetry (DSC) showed that both DiCP and SA increased the T_m of DMPC bilayers and broadened the phase transition (Figure 3), suggesting that the effects on *Bt*-PI-PLC activity may be explained in part by changes in fluidity of the bilayer as well as surface charge effects.

The reduced temperature of a lipid is defined as the experimental temperature minus the T_m of the lipid bilayer and is a measure of the fluidity of a bilayer (a high reduced temperature indicates high fluidity). A plot of the reduced temperature versus the activity of *Bt*-PI-PLC shows a good correlation between membrane fluidity and *Bt*-PI-PLC activity for all of the lipids tested in this study (Figure 4), supporting the proposal that lipid fluidity is a major determinant of *Bt*-PI-PLC activity.

Effect of Lipid Phase State on the Cleavage of 5′-NTase by Bt-PI-PLC. The activity of *Bt*-PI-PLC was determined with respect to temperature for cleavage of 5′-NTase in porcine lymphocyte plasma membrane vesicles, purified 5′-NTase reconstituted into proteoliposomes of DMPC, PMPC, and egg PC, and purified 5′-NTase solubilized in CHAPS. The data for each lipid system were summarized in Arrhenius plots (Figure 5), and values for the activation energy of anchor cleavage, E_{act}, were determined from the slopes (Table

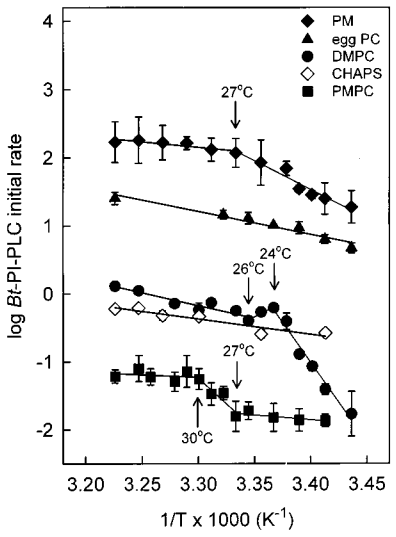

FIGURE 5: Arrhenius plots of the initial rate of *Bt*-PI-PLC cleavage of 5′-NTase in different lipid systems. Data are shown for lymphocyte plasma membrane vesicles (◆), purified 5′-NTase in CHAPS (◇), and reconstituted proteoliposomes of egg PC (▲), DMPC (●), and PMPC (■). Data points represent the mean ± SEM (n = 4); where not visible, error bars are included within the symbols.

Table 3: Activation Energies for *Bt*-PI-PLC Cleavage of 5′-NTase in Different Lipid Environments[a]

	temp range (°C)	E_{act} (kJ/mol^{-1})	r
lymphocyte plasma membrane vesicles	20−27	162 ± 18	0.972
	27−37	31 ± 8	0.891
DMPC	18−24	446 ± 35	0.988
	24−26	negative	0.982
	26−37	73 ± 11	0.946
PMPC	20−27	27 ± 13	0.782
	27−30	285 ± 80	0.929
	30−37	14 ± 23	0.293
egg PC	20−37	64 ± 7	0.974
CHAPS solution	20−37	44 ± 8	0.945

[a] Values for E_{act} in the different temperature ranges were calculated from the slopes of the lines in Figure 5. The correlation coefficient (r) indicates the goodness of fit to a straight line by linear regression analysis.

3). For cleavage of 5′-NTase in DMPC, there was a break in the Arrhenius plot at 24 °C (Figure 5) which corresponds to the melting temperature as determined by DSC (Figure 3). The E_{act} in the lower temperature range (18−24 °C) was 6-fold higher than the E_{act} in the higher temperature range (26−37 °C), where the membrane is in the fluid liquid crystalline phase (Table 3). It is interesting to note that there is also a measurable discontinuity in the data at 24−26 °C, just above the T_m of the bilayer. The slope of the plot is positive in this region, indicating that enzyme does not exhibit Arrhenius behavior in this temperature range. Calculation of E_{act} using the Arrhenius equation assumes that the constant A (which includes the activation entropy $\Delta S^{\ddagger}$) remains constant at different temperatures. Changes in $\Delta S^{\ddagger}$ arising from alterations in collisional frequency and orientation effects at different temperatures may therefore contribute to deviations from the Arrhenius equation. The apparent E_{act} value of 446 kJ/mol for DMPC in the gel phase is anomalously high and may be due to changes in $\Delta S^{\ddagger}$ arising from the lower collision frequency expected in the gel state.

As shown in Figure 5, porcine lymphocyte plasma membrane vesicles showed a break in the Arrhenius plot at 27 °C. The E_{act} in the lower temperature range was 5-fold greater than in the higher temperature range (see Table 3). DSC scans of lymphocyte plasma membrane vesicles showed that there was no thermotropic transition in the temperature range used in these experiments (Figure 3), so the break in the Arrhenius plot must arise from some other factor, possibly a change in $\Delta S^{\ddagger}$. It is also possible that temperature-dependent changes in membrane components other than lipids, such as other integral proteins, might affect packing of 5′-NTase and its accessibility to the phospholipase.

The cleavage of 5′-NTase was investigated in bilayers of PMPC (T_m = 30.5 °C, Figure 3), which differs from DMPC structurally in having one acyl chain of length increased by two carbon atoms. Surprisingly, PMPC showed a different Arrhenius plot pattern from DMPC. As shown in Figure 5, there is a break in the plot at 27 °C and a discontinuity in the data from 27 to 30 °C, just below the T_m. In contrast to the situation observed for DMPC, the plot has a negative slope in the region of the discontinuity, leading to a calculated E_{act} of 285 kJ/mol (Table 3). The value of E_{act} in the temperature range below 27 °C (gel phase) is 2-fold lower than that calculated above 30 °C (liquid crystalline phase).

Cleavage of solubilized 5′-NTase in CHAPS and 5′-NTase reconstituted into egg PC vesicles showed no breaks or discontinuities in the Arrhenius plots (Figure 5). The E_{act} values for these two systems were similar to those determined in the higher temperature ranges for 5′-NTase in lymphocyte plasma membrane vesicles and 5′-NTase reconstituted into DMPC (Table 3). Egg PC is in the fluid liquid crystalline phase over the temperature range used in these experiments (20−37 °C), so no melting transition would be expected.

Taken together, these results suggest that the phase state of the lipid bilayer modulates the catalytic properties of *Bt*-PI-PLC cleavage of the GPI anchor of 5′-NTase. For synthetic phospholipids, the E_{act} of anchor cleavage is higher when the bilayer is in the rigid gel phase and substantially lower when it is in the fluid liquid crystalline phase. This difference is larger for DMPC bilayers (6-fold) compared to PMPC bilayers (2-fold). Cleavage of 5′-NTase in both lipids shows complex behavior, with a discontinuity around the T_m of the bilayer.

Effect of Lipid Raft Components on the Cleavage of 5′-NTase by Bt-PI-PLC. Gangliosides are negatively charged glycosphingolipid components of lipid rafts (*40*−*42*) that may, therefore, affect *Bt*-PI-PLC cleavage activity by virtue of both their colocalization with GPI-anchored proteins and their negative charge. The addition of 5% (w/w) GM_1 to DMPC bilayers changed the slope of the Arrhenius plot compared to DMPC alone (Figure 6). The break in the Arrhenius plot occurred at a similar temperature in both cases (24 °C), and the discontinuity of positive slope remained, but there was a significant reduction in the E_{act} in both the gel phase (18−24 °C; ∼3-fold) and the liquid crystalline phase (26−37 °C; ∼2.2-fold) (Table 4). DSC showed that the addition of GM_1 broadened the phase transition of DMPC but did not alter the T_m substantially (Figure 3). The initial rate of *Bt*-PI-PLC cleavage at 37 °C was 4.4-fold lower for 5′-NTase in DMPC/5% GM_1 as compared to DMPC alone (Table 2); however, at 20 °C, the initial rate of cleavage was significantly higher in DMPC/5% GM_1. The headgroup of

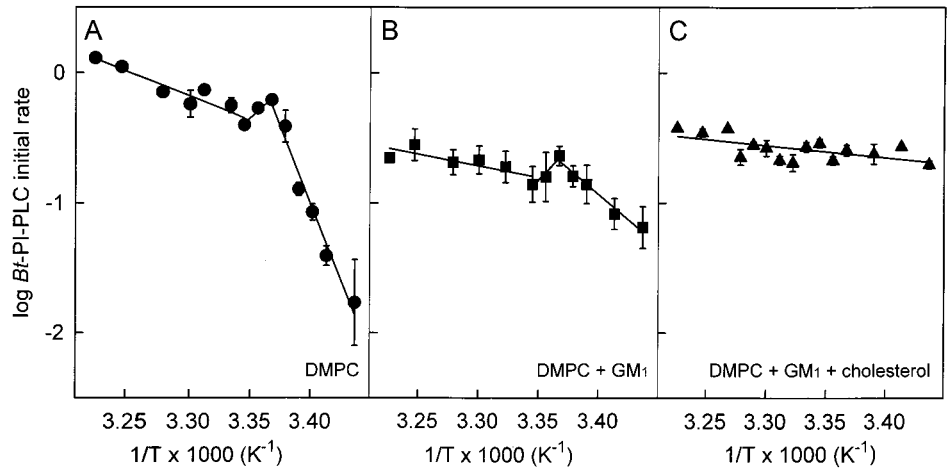

FIGURE 6: Effect of GM_1 and cholesterol on 5′-NTase cleavage by *Bt*-PI-PLC. Arrhenius plots of cleavage of purified 5′-NTase in (A) DMPC bilayers (●), (B) DMPC + 5% (w/w) GM_1 (■), and (C) DMPC + 5% (w/w) GM_1 + 22% (w/w) cholesterol (▲). Data points represent the mean ± SEM ($n = 2$); where not visible, error bars are included within the symbols.

Table 4: Activation Energies for *Bt*-PI-PLC Cleavage of 5′-NTase in DMPC Bilayers Containing Different Components[a]

	temp range (°C)	E_{act} (kJ/mol^{-1})	r
DMPC	18−24	446 ± 35	0.988
	24−26	negative	0.982
	26−37	73 ± 11	0.946
DMPC + 5% (w/w) GM_1	18−24	151 ± 15	0.993
	24−26	negative	0.965
	26−37	34 ± 12	0.902
DMPC + 5% (w/w) GM_1 + 22% (w/w) cholesterol	18−37	18 ± 6	0.624
DMPC + 10:1 (w/w) Thy-1	18−24	282 ± 37	0.975
	24−26	negative	0.998
	26−37	117 ± 16	0.962
SCRL	18−28	118 ± 7	0.981
	28−30	negative	0.988
	30−37	53 ± 22	0.811

[a] Values for E_{act} in the different temperature ranges were calculated from the slopes of the lines in Figures 5, 6, and 8. The correlation coefficient (r) indicates the goodness of fit to a straight line by linear regression analysis.

GM_1 has a single sialic acid residue, and it will thus add a negative charge to the bilayer equal to that of 5% DiCP but located further away from the surface. Yet 5% GM_1 enhanced anchor cleavage at 20 °C and reduced anchor cleavage at 37 °C, compared to the enhancement seen at both temperatures for DiCP. This disparity could be due to differences in bilayer packing between DMPC/5% GM_1 and DMPC/5% DiCP. To examine how gangliosides with multiple negative charges affected *Bt*-PI-PLC cleavage, 5′-NTase was reconstituted into DMPC vesicles containing 5% (w/w) of the trisialoganglioside, GT_{1b}. As seen in Table 2, GT_{1b} behaved very similarly to GM_1 in lowering the initial rate of cleavage in DMPC bilayers at 37 °C, indicating that a more negatively charged ganglioside does not further increase the inhibition of *Bt*-PI-PLC cleavage activity. These results suggest that packing effects, rather than surface charge, probably account for the effects of gangliosides on PI-PLC activity.

To determine whether DMPC bilayers containing 5′-NTase and gangliosides form rafts, or DRMs, we tested their solubility in ice-cold Triton X-100. Rafts/DRMs float at a characteristic low density and can be found in fractions 2−8 of a sucrose density gradient following cold Triton X-100 treatment. DRM fractions can be localized in the gradient using the activity of 5′-NTase, which is a raft marker. As seen in Figure 7, DMPC/5% GM_1 liposomes fail to form DRMs, as evidenced by the absence of 5′-NTase activity in fractions 2−8 of the sucrose density gradients. In contrast, SCRL, a synthetic lipid mixture known to mimic lipid rafts (*36*), was recovered in the DRM region of the gradient after cold Triton X-100 treatment (Figure 7). These results suggest that localization of 5′-NTase into DRMs does not contribute to the observed behavior of *Bt*-PI-PLC when cleaving the protein in bilayers of DMPC containing GM_1.

Cholesterol, along with sphingolipids, is considered a necessary component for the formation of lipid rafts (*8*, *43*) and can also influence the melting temperature of lipid bilayers. Incorporation of 22% (w/w) cholesterol into bilayers completely eliminated the break in the Arrhenius plot at 24 °C observed for DMPC/5% GM_1 (Figure 6). In fact, no break or discontinuity was evident over the entire temperature range. DSC confirmed that the phase transition of DMPC/5% GM_1 (w/w) was completely eliminated with the addition of 22% cholesterol (w/w) (Figure 3). The E_{act} was substantially lower (∼2-fold) for DMPC/5% GM_1/22% cholesterol (18−37 °C) when compared to the E_{act} for DMPC alone and DMPC/5% GM_1 (Table 4). The initial rate of cleavage by *Bt*-PI-PLC was increased for DMPC/5% GM_1/22% cholesterol as compared to DMPC/5% GM_1 at both 20 °C (∼3.3-fold) and 37 °C (∼1.7-fold) (Table 2). The cleavage rate at 20 °C is consequently only ∼30% lower than the rate at 37 °C, whereas in bilayers of DMPC alone, there is a 25-fold drop in the cleavage rate when moving from 37 °C (liquid crystalline phase) to 20 °C (gel phase). These results confirm that the phase state of the bilayer directly modulates *Bt*-PI-PLC activity; the rigid gel phase seems to be unfavorable for catalytic activity. Figure 7 shows that DMPC/5% GM_1/22% cholesterol bilayers also fail to form DRMs, as evidenced by the lack of 5′-NTase activity in fractions 2−8 of the sucrose gradients. This indicates that the effect of cholesterol on *Bt*-PI-PLC cleavage of 5′-NTase in DMPC/5% GM_1/22% cholesterol is not due to the formation of lipid rafts.

A recent study in our laboratory has shown that the GPI-anchored protein Thy-1 slightly broadens the gel to liquid

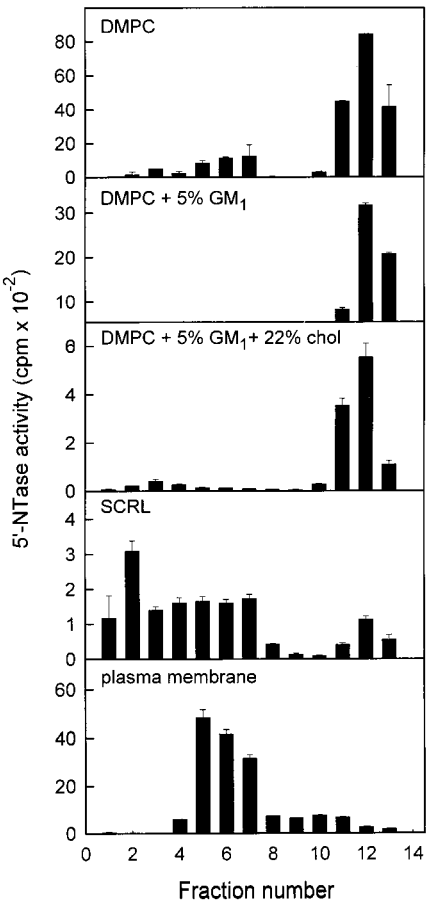

FIGURE 7: Formation of DRMs/rafts by the vesicle systems used in this study. Raft formation was assessed using the cold detergent insolubility of 5′-NTase, which is a raft marker. Lymphocyte plasma membrane vesicles and purified 5′-NTase in proteoliposomes of DMPC, DMPC + 5% (w/w) GM_1, DMPC + 5% (w/w) GM_1 + 22% (w/w) cholesterol, and SCRL were treated with 1% Triton X-100 at 4 °C for 30 min and subjected to sucrose density gradient centrifugation as described in Materials and Methods. Bars represent the 5′-NTase enzymatic activity ± SEM ($n = 3$) in the fractions collected from the sucrose gradient, determined by the radiometric assay described in Materials and Methods.

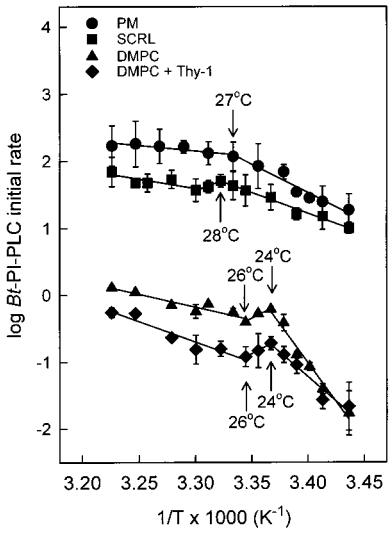

FIGURE 8: Effect of lipid raft components on the initial rate of *Bt*-PI-PLC cleavage of 5′-NTase. Arrhenius plots for cleavage of 5′-NTase in lymphocyte plasma membrane vesicles (●) and purified 5′-NTase in SCRL (■), DMPC (▲), and DMPC + 10:1 (w/w) Thy-1 (◆). Data points represent the mean ± SEM ($n = 4$); where not visible, error bars are included within the symbols.

crystalline phase transition of DMPC bilayers but has no effect on T_m (*37*). To investigate the effect of another GPI-anchored protein on *Bt*-PI-PLC cleavage, 5′-NTase was coreconstituted in DMPC bilayers containing 10:1 (w/w) Thy-1. Thy-1 had no effect on the break and discontinuity in the Arrhenius plot as compared to DMPC alone (Figure 8). However, the addition of Thy-1 lowered the E_{act} in the gel phase (18−24 °C; ∼1.6-fold) while increasing the E_{act} in the liquid crystalline phase (26−37 °C; ∼1.6-fold) (Table 4), suggesting that Thy-1 moderates the change occurring on melting of DMPC bilayers. The initial rate of cleavage of *Bt*-PI-PLC was similar for both systems at 20 °C but was reduced by a factor of ∼1.8 for DMPC/10:1 Thy-1 at 37 °C when compared to DMPC bilayers alone (Table 2). This reduction in activity may be due to a steric hindrance effect of surface-bound Thy-1 restricting access of the phospholipase to the 5′-NTase anchor or competition for 5′-NTase anchor cleavage by the Thy-1 anchor.

Sphingolipid/cholesterol-rich liposomes (SCRL) are known to form DRMs when treated with ice-cold nonionic detergents (*36*). The initial rate of cleavage of 5′-NTase in SCRL was quite high compared to DMPC and approached that observed for native lymphocyte plasma membrane. Both lymphocyte plasma membrane vesicles and SCRL formed DRMs when treated with cold Triton X-100 (Figure 7). *Bt*-PI-PLC cleavage of 5′-NTase in SCRL had a break point in the Arrhenius plot at 28 °C (Figure 8), which is similar to that seen for lymphocyte plasma membrane; however, there was also a discontinuity of positive slope for SCRL at 28−30 °C, which was not seen in lymphocyte plasma membrane. This discontinuity is similar to that seen at 24−26 °C for the DMPC-based lipid systems (Figure 8). SCRL showed a very broad melting transition starting at ∼28 °C by DSC (Figure 3), suggesting that the break and discontinuity in the Arrhenius plot may arise from melting of this lipid mixture, as with DMPC. The E_{act} for cleavage of 5′-NTase in SCRL is lower in the gel phase (18−28 °C; ∼1.4-fold) as compared to lymphocyte plasma membrane, but the E_{act} is similar in the liquid crystalline phase for both systems (Tables 3 and 4).

DISCUSSION

Release of mammalian GPI-anchored proteins by endogenous phospholipases may play an important role in regulation of their surface activity and also generates second messengers that initiate transmembrane signaling processes. Examining details of the activity of bacterial PI-PLCs toward GPI-anchored proteins may shed some light on the factors potentially regulating release of GPI-anchored proteins by endogenous phospholipases. Our approach in the present work was to use the purified GPI-anchored ectoenzyme 5′-NTase reconstituted into bilayer vesicles of defined phospholipids and to determine the effects on *Bt*-PI-PLC cleavage activity of membrane fluidity, acyl chain length, membrane surface charge, and the presence of lipid raft components. The reconstituted systems under study are all LUVs with a bimodal distribution of vesicle sizes. None are in the very small diameter range characteristic of SUVs or micelles, and they should not exhibit bilayer steric strain or high curvature. There was no correlation between the size ranges of the

various lipid vesicles and the cleavage activity of PI-PLC on the 5′-NTase substrate.

Bt-PI-PLC showed a high rate of cleavage activity toward the GPI anchor of 5′-NTase in bilayers of egg PC and DOPC bilayers as compared to DMPC and PMPC, indicating that membrane fluidity is important for *Bt*-PI-PLC activity. The cleavage activity of *Bt*-PI-PLC against 5′-NTase is highly correlated with the reduced temperature of the host lipid bilayer in which the GPI anchor is presented to the enzyme (Figure 4). Clearly, the higher the fluidity of the bilayer, the more active *Bt*-PI-PLC becomes toward the GPI anchor of 5′-NTase. Interfacial activation of phospholipases is a common phenomenon and depends on the physicochemical nature, as well as the organization and dynamics, of the interface. It has been studied quite extensively for phospholipase A_2 (reviewed in refs *23* and *24*) and other phospholipase enzymes (*25*). Several phospholipase A_2 enzymes appear to have a common "interfacial binding surface" (IBS) that is located on a flat external surface surrounding the active site (*44*). Bacterial PI-PLC displays interfacial activation toward both the membrane-bound substrate PI (*26*, *27*) and the water-soluble substrate cIP (*28*). It was suggested that binding to the membrane surface leads to allosteric activation of the enzyme. The crystal structure of PI-PLC from *Bacillus cereus* (*Bc*-PI-PLC), which is very closely related to *Bt*-PI-PLC, was determined alone and in a complex with *myo*-inositol or a fragment of the GPI anchor and has shed some light on the possible residues that make up the IBS (*45*, *46*). Helix 42−48 and loop 237−243 surround the rim of the active site pocket and contain an unusually high number of hydrophobic aliphatic and aromatic amino acids exposed to solvent. The helix and loop are highly flexible in the crystal structure, and they may adopt different conformations when bound to a membrane interface. Both the helix and the loop contain a Trp residue, and Trp fluorescence was shown to increase upon interfacial activation of *Bt*-PI-PLC by PC bilayers (*27*) and micelles (*28*). The hydrophobic and aromatic residues of the loop and helix of PI-PLC may penetrate into the bilayer and stabilize the membrane−protein complex, in a fashion similar to the model proposed for phospholipase A_2 (*47*). It may be easier for the hydrophobic residues of the *Bt*-PI-PLC enzyme to penetrate into a more fluid membrane, or the increased fluidity may stabilize the enzyme−bilayer complex, thus accounting for the increase in activity. The results presented in the current work are in agreement with this proposal. Also supporting this suggestion is the observation that *Bt*-PI-PLC is less active toward unilamellar vesicles of long-chain PI, which would be expected to be less fluid than short-chain PI (*29*). Also, *Bt*-PI-PLC is more active on PC micelles compared to more tightly packed PC vesicles (*29*), and substrate presentation in micelles rather than a bilayer leads to a higher apparent rate of hydrolysis by phospholipases in general (*48*). There was also less interfacial activation of *Bt*-PI-PLC when the enzyme encountered tightly packed, cross-linked PC molecules in unilamellar vesicles, as opposed to PC molecules in micelles (*28*).

Direct allosteric effects of individual lipid molecules on the phospholipase could possibly account for some of the observations reported in the present study. Zhou et al. (*29*) investigated whether *Bt*-PI-PLC activation toward cleavage of the soluble substrate cIP arose from interaction with a single phospholipid or whether the phospholipid was required to be part of a surface. Monomeric short-chain PC, which did not form micelles at the concentration at which it was used, gave very low PI-PLC activation compared to PC species that formed micelles, and the level of activation correlated well with the critical micelle concentration (*29*). Thus they concluded that the optimal allosteric activator was a PC molecule presented at an interface. Binding to this surface via a lipid-specific allosteric site altered the enzyme conformation to increase its catalytic activity (*28*), possibly by allowing partial penetration of the enzyme into the hydrophobic core (see above). Binding of a single lipid molecule was not sufficient to convert PI-PLC to the active form; an interface was necessary to drive the conformational change. Thus it seems likely that the large variations in *Bt*-PI-PLC activity observed in the present study arise primarily from the physical properties of the bilayer surface, rather than the chemical nature of the individual phospholipid molecules.

In the present study, a high rate of *Bt*-PI-PLC cleavage was also associated with lipid bilayers and membranes that form rafts (SCRL, native plasma membrane). This may be explained by the higher local concentration of substrate (5′-NTase) as a result of clustering into the lipid raft microdomains. It has been suggested that bacterial PI-PLC acts on substrate in the processive "scooting mode" of interfacial catalysis, where the enzyme stays bound to the membrane for multiple catalytic turnover cycles, up to 40−50 catalytic cycles per binding event (*27*). If the substrate is concentrated into membrane rafts, more catalytic turnover cycles could occur per binding event due to a higher local concentration of substrate.

The effect of temperature on the cleavage of 5′-NTase by *Bt*-PI-PLC was assessed by constructing Arrhenius plots of anchor cleavage in various lipid bilayers. The breaks in the Arrhenius plots correlated with bilayer phase transitions in every case, except for lymphocyte plasma membrane. A change in $\Delta S^{\ddagger}$ might account for the observed break in the Arrhenius plot in this instance and also for the anomalously high values of E_{act} measured at lower temperatures, where membrane bilayers are in the rigid gel phase. Since $\Delta S^{\ddagger}$ is a function of the collision frequency, Z, a radical change in Z might be expected in the gel phase. The E_{act} of anchor cleavage was higher in the gel phase for all of the lipid bilayers analyzed, indicating that the rigid gel phase is unfavorable for catalytic activity of *Bt*-PI-PLC. As discussed above, it may be more difficult for the hydrophobic sequences of the IBS of the enzyme to penetrate the rigid gel phase, since it has tighter packing density and low surface deformability. When cholesterol was added to the DMPC bilayer, it abolished the phase transition and had a dramatic effect on *Bt*-PI-PLC activity. In the presence of cholesterol, the cleavage rate at 20 °C was only ∼30% lower than the rate at 37 °C, whereas in bilayers of DMPC alone, there was a 25-fold drop in the cleavage rate when moving from 37 °C (liquid crystalline phase) to 20 °C (gel phase). Cholesterol both increases the fluidity of the gel phase and decreases the fluidity of the liquid crystalline phase, thus smoothing out the changes in fluidity that would normally occur over this temperature range. These results confirm the effects of lipid fluidity and bilayer phase state on *Bt*-PI-PLC activity.

The values of E_{act} presented in Tables 3 and 4 vary considerably. We cannot rule out the possibility that the phospholipase enzyme is not always saturated with 5′-NTase substrate over the wide temperature range used in this study, since it is not possible to determine this when the substrate is part of a membrane vesicle system. Estimates of K_M and V_{max} have been made using PI in micelles, as well as GPI-anchored substrates in mixed micelles of detergent and phospholipid (*49*). The K_M value at 25 °C for GPI-anchored substrates was substantially lower than that for PI (7−17 μM vs 2 mM), suggesting that the phospholipase is likely to be saturated with substrate in the vesicle systems we have used at 25 °C. However, the temperature dependence of K_M has not been investigated. Altered surface binding of the PI-PLC might also affect the observed kinetics of cleavage. This could perhaps account for the anomalously high E_{act} values observed for DMPC in the gel phase; however, gel phase PMPC does not display an extraordinarily high E_{act}.

Negatively charged DiCP slightly increased the activity of *Bt*-PI-PLC, whereas positively charged SA substantially reduced the phospholipase activity in DMPC bilayers. Electrostatics plays a vital role in the activity of phospholipase A_2 by stabilizing the enzyme−membrane complex (*23*, *47*). Cationic residues in the IBS of this phospholipase interact with anionic residues in the bilayer. However, membrane surface charge appears to have only small effects on PI-PLC activity and surface binding. It was reported that *Bc*-PI-PLC has similar affinity for micelles of anionic and zwitterionic phospholipids (*27*). Although the overall charge of *Bt*-PI-PLC at physiological pH is negative (*35*; Oxford Glycosciences Inc., Bedford, MA), the electrostatic potential of the IBS of the related enzyme *Bc*-PI-PLC (helix 42−48 and loop 237−243) is positive, due to the presence of Lys44 (electrostatic potential calculated using Rasmol version 2.7.1.1, PDB 1GYM). *Bt*-PI-PLC has a Lys residue in the same position (*50*), which is likely also to be located in the IBS. Interfacial activation of PI-PLC may, therefore, occur through both electrostatic and nonpolar interactions of the IBS with the membrane. Positively charged vesicles containing SA may inhibit the activation of the IBS due to its positive electrostatic potential, whereas a negatively charged bilayer surface containing DiCP may enhance interfacial activation. However, these effects are small compared to those noted for phospholipase A_2, which has several highly basic clusters of residues, resulting in an increase of several orders of magnitude in affinity for vesicles of anionic vs zwitterionic vesicles. Differences in the degree of activation of *Bt*-PI-PLC at 20 and 37 °C suggest that packing/fluidity may also contribute to the effects of DiCP and SA. Taken together, these observations suggest that changes in *Bt*-PI-PLC activity caused by DiCP and SA may arise from both charge effects and differences in the packing/fluidity of the bilayer.

The fact that GM_1 (one negative charge) has the same effect as GT_{1b} (three negative charges) on anchor cleavage by *Bt*-PI-PLC supports the proposal that the magnitude of the surface charge does not seem to have a substantial effect on the enzyme activity. Again, the measured effects of gangliosides on anchor cleavage may be due to differences in bilayer packing/fluidity, or they could arise from direct effects on the phospholipase enzyme itself. Gangliosides are known to inhibit the activity of a variety of lipolytic enzymes including nonspecific PI-PLC from *B. cereus* (*51*) and *Clostridium perfringens* (*52*, *53*), type I PLA_2 from porcine pancreas (*54*, *55*), and type II PLA_2 from snake venom (*56*). The proposed mechanism of inhibition in these cases is thought to be through direct alteration of the adsorbed phospholipase and/or by altering the availability of substrate at the membrane surface through steric interactions (*51*). These factors may also contribute to inhibition of *Bt*-PI-PLC cleavage by gangliosides. E_{act} is the same in the presence of gangliosides as in their absence (in both the gel and liquid crystalline phases), which indicates that the energy barrier for anchor cleavage is not affected by the presence of the glycolipids. This suggests that gangliosides do not affect the overall intrinsic mechanism of catalysis by *Bt*-PI-PLC. They may affect adsorption of the phospholipase to the membrane surface via packing/fluidity effects. Gangliosides have long acyl chains and are less fluid than the DMPC bilayer, and they may, therefore, decrease the adsorption rate or increase the desorption rate of *Bt*-PI-PLC from the bilayer surface. Gangliosides may also have a steric effect by virtue of their large oligosaccharide headgroups, decreasing the access of *Bt*-PI-PLC to the substrate in the membrane interfacial region.

The presence of the GPI-anchored protein, Thy-1, in the lipid bilayer reduced the overall activity of *Bt*-PI-PLC. However, as in the case of gangliosides, the E_{act} was unchanged, suggesting that the overall intrinsic mechanism of catalysis was unaffected. The packing/fluidity of DMPC bilayers was not changed significantly in the presence of 10:1 (w/w) Thy-1 (*37*), which is expected, since the mole fraction will be very small compared to 5% GM_1 (w/w). The reduced activity observed in the presence of Thy-1 may be due to steric effects, as suggested above for gangliosides, or competition for 5′-NTase anchor cleavage by the Thy-1 anchor.

The IBS of phospholipase A_2 has been studied extensively by site-directed mutagenesis to identify the residues important in the membrane-binding process. Although the proposed IBS for bacterial PI-PLC has been elucidated from the crystal structure, little work has been done to identify the amino acid residues that are responsible for membrane binding and interfacial activation. Site-directed mutagenesis studies are needed to confirm the results of the present study, which support the view that the residues of the IBS of PI-PLC that penetrate the membrane bilayer are bulky nonpolar side chains, rather than charged amino acids.

REFERENCES

1. Ferguson, M. A. J. (1999) *J. Cell Sci. 112*, 2799−2809.
2. Zhou, F. X., Merianos, H. J., Brunger, A. T., and Engelman, D. M. (2001) *Proc. Natl. Acad. Sci. U.S.A. 98*, 2250−2255.
3. Hooper, N. M. (1997) *Clin. Chim. Acta 266*, 3−12.
4. McConville, M. J., and Ferguson, M. A. (1993) *Biochem. J. 294*, 305−324.
5. Noda, M., Yoon, K., Rodan, G. A., and Koppel, D. E. (1987) *J. Cell Biol. 105*, 1671−1677.
6. Brown, D. A., and Rose, J. K. (1992) *Cell 68*, 533−544.
7. Tooze, S. A., Martens, G. J. M., and Huttner, W. B. (2001) *Trends Cell Biol. 11*, 116−122.
8. Simons, K., and Ikonen, E. (1997) *Nature 387*, 569−572.
9. Brown, D. A., and London, E. (2000) *J. Biol. Chem. 275*, 17221−17224.
10. Cary, L. A., and Cooper, J. A. (2000) *Nature 404*, 945−947.

11. Langlet, C., Bernard, A. M., Drevot, P., and He, H. T. (2000) *Curr. Opin. Immunol. 12*, 250−255.
12. Hoessli, D. C., Ilangumaran, S., Soltermann, A., Robinson, P. J., Borisch, B., and Din, N. U. (2000) *Glycoconjugate J. 17*, 191−197.
13. Katagiri, Y. U., Kiyokawa, N., and Fujimoto, J. (2001) *Microbiol. Immunol. 45*, 1−8.
14. Fantini, J., Maresca, M., Hammache, D., Yahi, N., and Delézay, O. (2000) *Glycoconjugate J. 17*, 173−179.
15. Fivaz, M., Abrami, L., and Van der Goot, F. G. (2000) *Protoplasma 212*, 8−14.
16. Rhee, S. G., Suh, P. G., Ryu, S. H., and Lee, S. Y. (1989) *Science 244*, 546−550.
17. Ferguson, M. A., Homans, S. W., Dwek, R. A., and Rademacher, T. W. (1988) *Science 239*, 753−759.
18. Ikezawa, H. (1991) *Cell Biol. Int. Rep. 15*, 1115−1131.
19. Low, M. G. (1981) *Methods Enzymol. 71*, 741−746.
20. Marques, M. B., Weller, P. F., Parsonnet, J., Ransil, B. J., and Nicholson-Weller, A. (1989) *J. Clin. Microbiol. 27*, 2451−2454.
21. Camilli, A., Goldfine, H., and Portnoy, D. A. (1991) *J. Exp. Med. 173*, 751−754.
22. Mengaud, J., Braun-Breton, C., and Cossart, P. (1991) *Mol. Microbiol. 5*, 367−372.
23. Gelb, M. H., Cho, W., and Wilton, D. C. (1999) *Curr. Opin. Struct. Biol. 9*, 428−432.
24. Jain, M. K., and Berg, O. G. (1989) *Biochim. Biophys. Acta 1002*, 127−156.
25. Roberts, M. F. (1996) *FASEB J. 10*, 1159−1172.
26. Lewis, K. A., Garigapati, V. R., Zhou, C., and Roberts, M. F. (1993) *Biochemistry 32*, 8836−8841.
27. Volwerk, J. J., Filthuth, E., Griffith, O. H., and Jain, M. K. (1994) *Biochemistry 33*, 3464−3474.
28. Zhou, C., Qian, X., and Roberts, M. F. (1997) *Biochemistry 36*, 10089−10097.
29. Zhou, C., Wu, Y., and Roberts, M. F. (1997) *Biochemistry 36*, 347−355.
30. Lehto, M. T., and Sharom, F. J. (1998) *Biochem. J. 332*, 101−109.
31. Maeda, T., Balakrishnan, K., and Mehdi, S. Q. (1983) *Biochim. Biophys. Acta 731*, 115−120.
32. Peterson, G. L. (1977) *Anal. Biochem. 83*, 346−356.
33. Loe, D. W., Glover, J. R., Head, S., and Sharom, F. J. (1989) *Biochem. Cell Biol. 67*, 214−223.
34. Sharom, F. J., Lorimer, I., and Lamb, M. P. (1985) *Can. J. Biochem. Cell Biol. 63*, 1049−1057.
35. Sharom, F. J., McNeil, G. L., Glover, J. R., and Seier, S. (1996) *Biochem. Cell Biol. 74*, 701−713.
36. Schroeder, R., London, E., and Brown, D. A. (1994) *Proc. Natl. Acad. Sci. U.S.A. 91*, 12130−12134.
37. Reid-Taylor, K. L., Chu, J. W. K., and Sharom, F. J. (1999) *Biochem. Cell Biol. 77*, 189−200.
38. Kume, T., Taguchi, R., Tomita, M., Tokuyama, S., Morizawa, K., Nakachi, O., Hirano, J., and Ikezawa, H. (1992) *Chem. Pharm. Bull. (Tokyo) 40*, 2133−2137.
39. Bordier, C. (1981) *J. Biol. Chem. 256*, 1604−1607.
40. Prinetti, A., Iwabuchi, K., and Hakomori, S. (1999) *J. Biol. Chem. 274*, 20916−20924.
41. Sheets, E. D., Lee, G. M., Simson, R., and Jacobson, K. (1997) *Biochemistry 36*, 12449−12458.
42. Simons, M., Friedrichson, T., Schulz, J. B., Pitto, M., Masserini, M., and Kurzchalia, T. V. (1999) *Mol. Biol. Cell 10*, 3187−3196.
43. Cerneus, D. P., Ueffing, E., Posthuma, G., Strous, G. J., and van der Ende, A. (1993) *J. Biol. Chem. 268*, 3150−3155.
44. Scott, D. L., and Sigler, P. B. (1994) *Adv. Protein Chem. 45*, 53−88.
45. Heinz, D. W., Ryan, M., Bullock, T. L., and Griffith, O. H. (1995) *EMBO J. 14*, 3855−3863.
46. Heinz, D. W., Ryan, M., Smith, M. P., Weaver, L. H., Keana, J. F., and Griffith, O. H. (1996) *Biochemistry 35*, 9496−9504.
47. Stahelin, R. V., and Cho, W. H. (2001) *Biochemistry 40*, 4672−4678.
48. Roberts, M. F., and Dennis, E. A. (1989) in *Phosphocholine Metabolism*, CRC Press, Boca Raton, FL.
49. Stieger, S., and Brodbeck, U. (1991) *Biochimie 73*, 1179−1186.
50. Lechner, M., Kupke, T., Stefanovic, S., and Gotz, F. (1989) *Mol. Microbiol. 3*, 621−626.
51. Daniele, J. J., Maggio, B., Bianco, I. D., Goni, F. M., Alonso, A., and Fidelio, G. D. (1996) *Eur. J. Biochem. 239*, 105−110.
52. Bianco, I. D., Fidelio, G. D., and Maggio, B. (1990) *Biochim. Biophys. Acta 1026*, 179−185.
53. Bianco, I. D., Fidelio, G. D., Yu, R. K., and Maggio, B. (1991) *Biochemistry 30*, 1709−1714.
54. Bianco, I. D., Fidelio, G. D., and Maggio, B. (1989) *Biochem. J. 258*, 95−99.
55. Maggio, B., Bianco, I. D., Montich, G. G., Fidelio, G. D., and Yu, R. K. (1994) *Biochim. Biophys. Acta 1190*, 137−148.
56. Daniele, J. J., Bianco, I. D., and Fidelio, G. D. (1995) *Arch. Biochem. Biophys. 318*, 65−70.

BI011579W